Journal of Molecular Graphics and Modelling 27 (2009) 590–599

Contents lists available at ScienceDirect

Journal of Molecular Graphics and Modelling

journal homepage: www.elsevier.com/locate/JMGM

Application of the independent molecule model to elucidate the dynamics of structure I methane hydrate: A third report

Shuzo Yoshioki *

Yatsushiro National College of Technology, Yatsushiro, 866-8501, Japan

ARTICLE INFO

Article history:
Received 15 July 2008
Received in revised form 17 September 2008
Accepted 22 September 2008
Available online 5 October 2008

Keywords:
Methane hydrate SI
Dynamics
Vibrational frequency
Independent molecule model
Surface water fixed method
Raman spectrum
Hydrogen bond
Bond stretching mode
Thermal ellipsoid

ABSTRACT

Two new model systems of methane hydrate, larger than the previous systems, are constructed. One consists of 63 small and large cages with a small cage at the centre. The other has 65 small and large cages with a large cage at the centre. Three different H-bonding network patterns between water are formed, and three random orientations of methane in each cage are chosen. Using the surface water fixed method, we obtained the energy minimum conformations, fitted to the X-ray crystallographic structure. With normal mode analysis, we calculated frequencies of 2915.1 cm^{-1} for a small cage, and 2911.0 cm^{-1} for a large cage. These frequencies are a little nearer to the Raman spectra than were previous model systems. Treating three force constants of anharmonic potential energy and the strength of H-bonding between methane and water as four parameters, we obtained frequencies of 2913.6 cm^{-1} for a small cage, a little lower than the Raman, and 2906.6 cm^{-1} for a large cage, a little higher than the Raman. The calculations thus almost reach the Raman spectra.

1. Introduction

In our two earlier papers on the independent molecule model [1,2], we demonstrated the dynamical vibrations of methane as a guest molecule in ice-like hydrogen bonded cages. Hereinafter these two papers are referred to as the 1st and the 2nd papers, respectively.

First, we briefly summarize the 1st paper [1]. As a model system of methane hydrate, referred to as an M2 system hereinafter, we picked a dodecahedra, formed by 12 pentagons designated 5^{12} (a small cage), and a tetrakaidecahedra, formed by 12 pentagons and 2 hexagons designated $5^{12}6^2$ (a large cage) [3,4]. These cages are in contact, and each holds one methane. Raman spectroscopy gives the C–H stretch (A1 mode) frequency ν_1 of hydrated methanes at 2915 cm^{-1} for the small cage and 2905 cm^{-1} for the large cage [5–7]. These values are lower than the frequency of 2916.5 cm^{-1} in gaseous methane. In the 1st paper, the theory led to 2915.4 cm^{-1} for the small cage, and 2901.9 cm^{-1} for the large cage. Our results are thus in reasonable agreement with observed Raman spectra when we include the cubic anharmonic terms in addition to the harmonic terms in the potential energy calculation on methane [8,9] and include the hydrogen bonding (H-bonding) energy between methane hydrogen and water oxygen. For this H-bonding strength, we used 75% of the strength of the H-bonding potential energy between waters.

Next, we summarize the 2nd paper [2]. We extended the M2 system of the 1st paper and constructed two model systems. One was constructed with a small cage surrounded by 12 large cages. Each of the 13 cages holds one methane. This model with a small cage at a centre of the system was called an M13 system hereinafter. The second model had a large cage surrounded by 4 small cages and 10 large cages. Each of the 15 cages holds one methane. This model with a large cage at a centre was called an M15 system. Initial orientations of each methane in both model systems were created randomly, and appropriate H-bonding networks between waters forming cages were constructed in both model systems. In order to put methanes in as different environments as possible, we made three different H-bonding network patterns between water molecules in both the M13 and M15 systems, in addition to three different orientations of each methane in the cages. That is, one network pattern of hydrogen bond has three different orientations of methanes. Thus, each methane was put in nine different environments in M13 and M15, respectively. The combinations of networks and orientations are called assemblies. Each of the nine assemblies of the M13 and M15 systems was energy minimized. We realized that the H-bondings

* Tel.: +81 965 53 1309; fax: +81 965 53 1319.
E-mail address: yoshioki@as.yatsushiro-nct.ac.jp.

1093-3263/$ – see front matter © 2008 Elsevier Inc. All rights reserved.
doi:10.1016/j.jmgm.2008.09.012

between methane and water deformed the cages during energy minimizatins. Such deformed cages could not correspond to the structures found in nature. Hence we suggested a new method called surface water fixed method, which should be based on two characteristics. One is that the structure of the methane hydrate must be close to the X-ray crystallographic structure. The other is that molecules in the model system should be allowed to move as freely as possible. Thus only oxygens of waters forming the surface of the model system were fixed, and the other atoms in the model system were allowed to move freely. With this method, we minimized the energy of each of the nine assemblies of the M13 and M15 systems. As a result, we found the frequencies of A1 mode were lower than the ones calculated by the minimization with no constraints so far used and were a little closer to the experimental Raman spectra. We proposed in the 2nd paper that if we could construct a model system vastly larger than the M13 and M15 systems, it would be possible to get frequencies in good agreement to the Raman spectra.

The main purpose of the present article is to construct a model system as large as possible to see if we can better predict the observed Raman Spectra.

In Section 2, the method of the independent molecule model and the potential energy E for methane hydrate are briefly described. See Refs. [1,2] for the details. In Section 3, new model systems adopted are represented. The results are given in Section 4. Discussion and conclusion are in Section 5.

2. Method

The essential point of the independent molecule model which has been applied in our earlier papers is to separate the motions of each molecule in the system into the rigid-body motion (with six degrees of freedom) and the internal motions; the variables describing movements as a rigid body are a translational vector and Eulerian angles specifying position and orientation of each molecule. As the variables describing internal movements within molecule, four bond lengths and six bond angles are chosen for methane, while two bond lengths and one bond angle are for water molecules.

As the total potential energy E of methane hydrate, the following five energies are chosen (for the details see Ref. [1]):

$$E = E_{\mathrm{wat}} + E_{\mathrm{wat-wat}} + E_{\mathrm{met}} + E_{\mathrm{met-met}} + E_{\mathrm{met-wat}} \tag{1}$$

The first energy E_{wat} is an intramolecular interaction of water. The second energy $E_{\mathrm{wat-wat}}$ is an intermolecular interaction between waters. The third energy E_{met} is an intramolecular interaction of methane and is expressed as below:

$$E_{\mathrm{met}} = \sum_{\mathrm{methanes}} \{V^{(2)} + V^{(3)}\} \tag{2}$$

where $V^{(2)}$ describes a harmonic potential energy and $V^{(3)}$ is the cubic anharmonic potential energy. The fourth energy $E_{\mathrm{met-met}}$ is an intermolecular interaction between methanes. The fifth energy $E_{\mathrm{met-wat}}$ is an intermolecular interaction between methane and water and is expressed as below:

$$E_{\mathrm{met-wat}} = \sum_{\mathrm{pairs}} \frac{1}{4\pi\varepsilon_0} \frac{q_i q_j}{r_{ij}} + \sum_{\mathrm{pairs}} \left\{ \varepsilon \left(\frac{r_0}{r_{ij}} \right)^{12} - 2\varepsilon \left(\frac{r_0}{r_{ij}} \right)^{6} \right\} + \sum_{\mathrm{H-bonds}} \left\{ \varepsilon \left(\frac{r_0}{r_{HX}} \right)^{12} - 2\varepsilon \left(\frac{r_0}{r_{HX}} \right)^{10} \right\} \tag{3}$$

where the parameter values are given in Table 3 of the 1st paper.

The second derivatives of the total potential energy are quantities necessary for doing energy minimization of methane hydrate system and then for doing normal mode analysis. These are expressed in a single equation as follows:

$$\frac{\partial^2 E}{\partial q_i \partial q_j} = (\Phi_i, \psi_i) \left\{ s_{ij} \sum_{\xi \in M_i} \sum_{\eta \in M_j} \left(c_{\xi\eta} C^*_{ij} + d_{\xi\eta} D_{\xi\eta} \right) \right\} \begin{pmatrix} \Phi_j \\ \psi_j \end{pmatrix} \tag{4}$$

Here q_i means the independent variables of each molecule in methane hydrate. See the 2nd paper for the derivation of Eq. (4).

3. New modelling of methane hydrate

3.1. Construction of M63 and M65 systems

Construction of the new larger model systems beyond the model M13 and M15 systems of the 2nd paper is done as follows. The M13 system is further surrounded with 14 small cages and 36 large cages. This model system totals 63 cages, each of which holds one methane, which is referred to as an M63 system. This is depicted in Fig. 1(a and b). The M15 system is further surrounded with 12 small cages and 38 large cages. This system totals 65 cages, each of which holds one methane, and is referred to as an M65 system. This system is depicted in Fig. 2(a and b). These model systems including the model M13 and M15 systems are summarized in Table 1.

3.2. Three hydrogen-bonding networks

As illustrated in Figs.1(b) and 2(b), we constructed a proper H-bonding network between water molecules in both the M63 and M65 systems, in addition to the methanes configured randomly in each cage. In order to put methanes in as different environments as possible, as done in the 2nd paper, we constructed three different H-bonding network patterns between water molecules in both the M63 and M65 systems, in addition to using three different orientations of each methane in the cages. We use the same terminology as in the 2nd paper: in both the M63 and M65 systems, the first H-bonding network pattern (1st network) has three randomly determined initial orientations of methanes (ran1, ran2 and ran3). A 2nd network has also ran1, ran2 and ran3 orientations. A 3rd network has ran1, ran2 and ran3. The combinations of networks and orientations are called assemblies. As an example for the M63 system, we depict in Fig. 3(a) stereo drawings of the 1st network with ran1 orientation and the 2nd network with ran2 orientation. Also an example for the M65 system is drawn in Fig. 3(b).

4. Results

4.1. Energy minimization both for M63 and M65 systems

Each of the nine assemblies for the M63 system is energy minimized using Newton's method based on a modified Cholesky factorization of the Hessian [10]. Each assembly consists of 63 cages (624 waters) and 63 methanes. The number of degrees of freedom is 6624 {624×9 and $63 \times (15 + 1)$}; see Ref. [1]. As suggested in the 2nd paper, the energy minimization uses the surface water fixed method. The goal of the method is to obtain energy minimized conformation fitted to the X-ray crystallographic structure. Thus we prevent movements of oxygens on or near to the surface of the system. In the case of the M63 system, oxygens forming the 50 cages newly added to the M13 system, figured in Fig. 1(b), are fixed. But hydrogens linked to these oxygens can be allowed to move. That is, waters with these oxygens have three degrees of freedom of Eulerian angles specifying orientation as a rigid-body motion of water and three

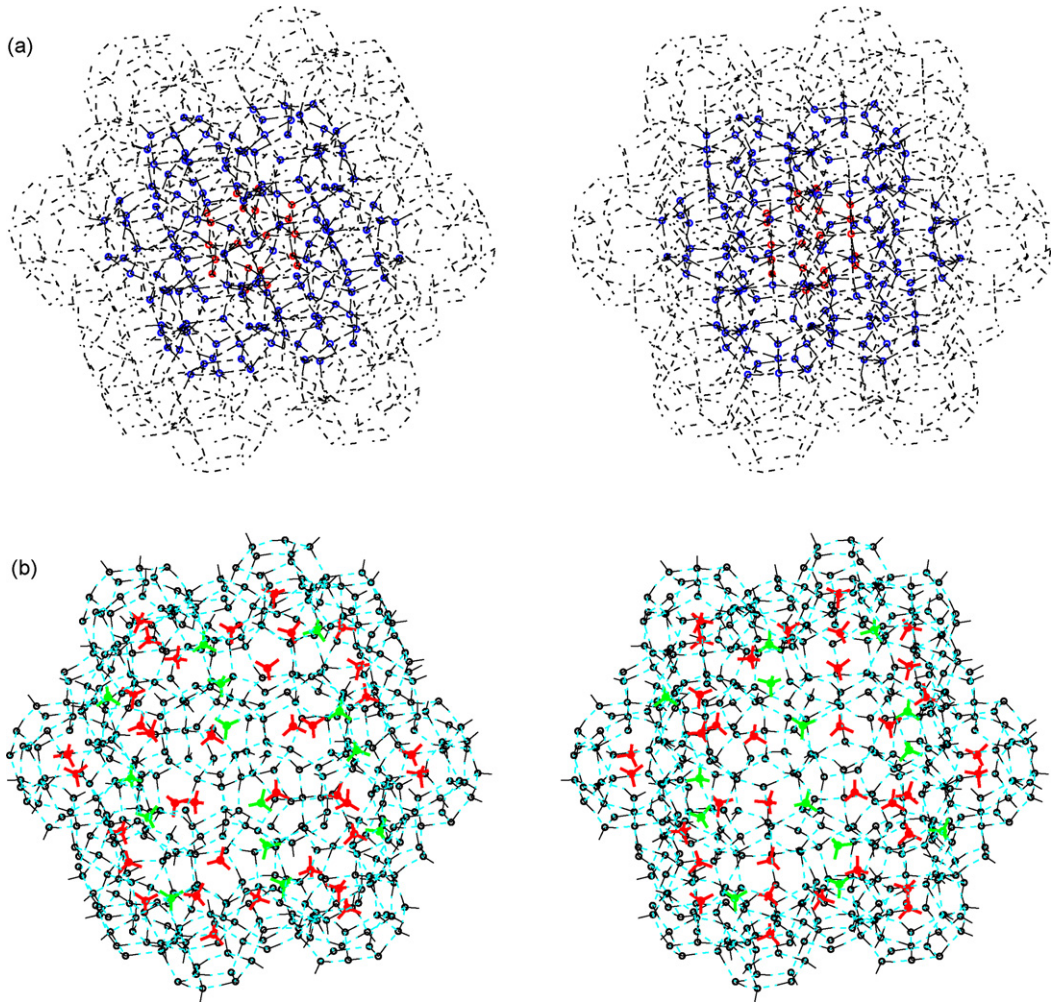

Fig. 1. Stereo view for the M63 system. (a) The M13 system is coloured with the central small cage in red and the other 12 cages in blue. The 50 cages added to the M13 system are in black. (b) Only the 50 cages added are drawn. Methanes in small cages are in green, while those in large cages are in red.

degrees of freedom of internal motions. The other waters (i.e., the 172 waters forming only the M13 system within the M63 system) and all the 63 methanes are allowed to move freely. The total potential energy E of Eq. (1) with the harmonic and anharmonic potential energy in Eq. (2) and with the H-bonding potential between methane and water in Eq. (3) is used for minimization. For the H-bonding potential energy between methane and water, we assume the strength to be 75% of the strength between waters as was done in the 1st and the 2nd papers. The dielectric constant between methanes is set to *in vacuo* value ε_0. Energy minimization is stopped when the energy difference between the current step and the earlier step becomes less than 1.0×10^{-26} aJ. As found in the 2nd paper, at the energy minimum point, six positive eigenvalues for each subset of the Hessian expressed in terms of variables of a rigid-body motion for the respective methanes and waters could not be obtained because of the constraints on the fixed waters. But we could get 10 positive eigenvalues of the respective methanes and three positive eigenvalues of the respective waters for each subset of the Hessian expressed in terms of internal variables.

Table 1
Constitution of model systems.

M13 system	M63 system
One central small cage, 12 large cages	One central small cage, 12 large cages
	14 small cages added, 36 large cages added
172 water molecules present	624 water molecules present
M15 system	**M65 system**
One central large cage, 4 small cages, 10 large cages	One central large cage, 4 small cages, 10 large cages 12 small cages added, 38 large cages added
184 water molecules present	628 water molecules present

Similarly, energy minimization was performed on each of the nine assemblies of the M65 system. The system consists of 65 cages (628 waters) and 65 methanes. The number of degrees of freedom is 6692{628 $\times$ 9 and 65 $\times$ (15 + 1)}. Fixed oxygens in the M65 system are oxygens of waters forming 50 cages newly added to the M15 system, shown in Fig. 2(b), while the other waters (i.e., the 184 waters forming the M15 system within the M65 system) and all 65 methanes are allowed to move freely. Likewise, we obtained the respective positive eigenvalues for each subset of the Hessian.

4.2. Normal mode analysis of methanes both for M63 and M65 systems

The force constant matrix necessary to do normal mode analysis is the subset of the Hessian for each methane in the energy

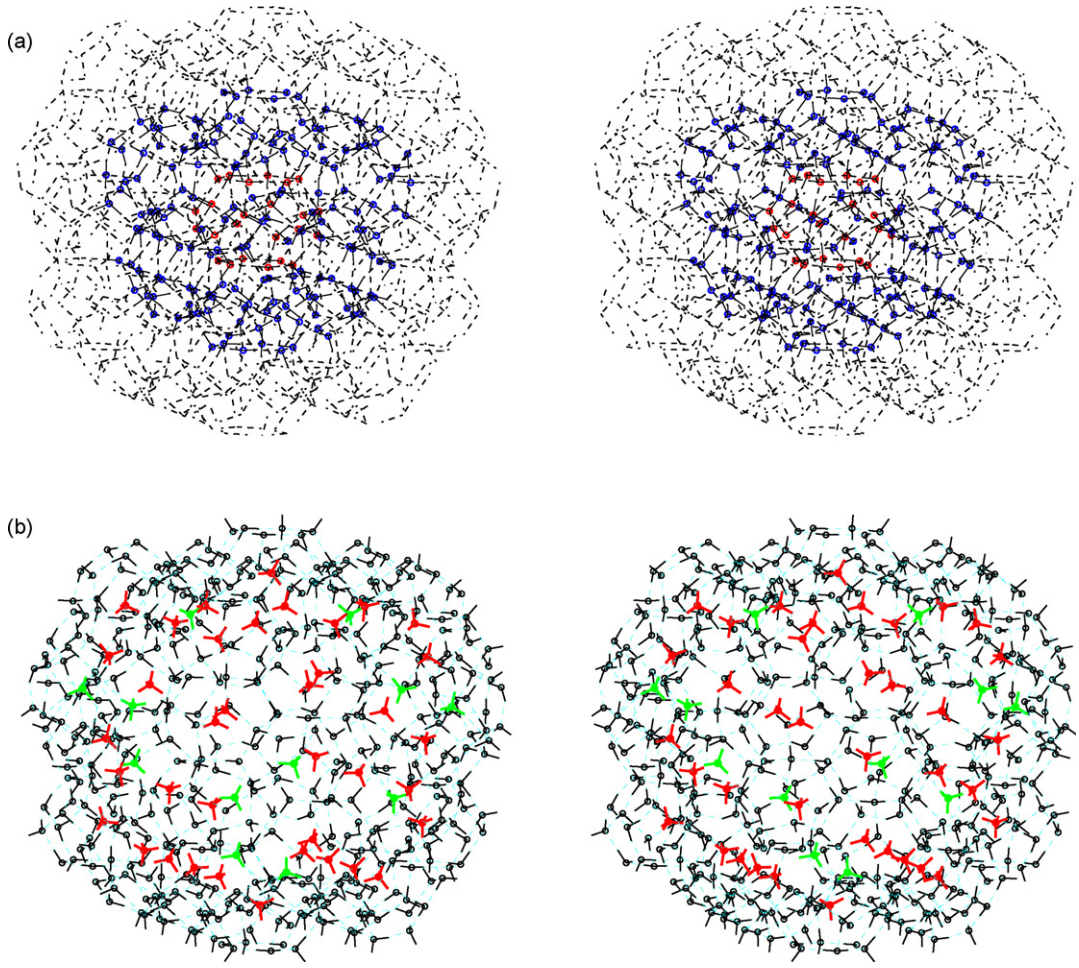

Fig. 2. Stereo view for the M65 system. (a) The M15 system is coloured with the central large cage in red and the other 14 cages in blue. The 50 cages added to the M15 system are in black. (b) Only the 50 cages added are drawn. Methanes in small cages are in green, while those in large cages are in red.

minimum conformation and has 10 positive eigenvalues. The kinetic energy matrix is given in Ref. [1]. Using the symmetry coordinates, these matrices with 10×10 elements are reduced to matrices with 9×9 elements. With the force constant and the kinetic energy matrices, nine normal vibrational frequencies for each methane both in the M63 and M65 systems were obtained. See Ref. [1].

We focus only on the C–H stretch (A1 mode) frequency ν_1 of each methane. In Fig. 4(a and b), we show histograms of frequency ν_1 of the A1 mode considering three H-bonding network patterns and three random orientations for the M63 and M65 systems. Since each methane in the cages experiences nine different environments of three H-bonding network patterns with three random orientations, and since the C–H stretch frequency of each methane in the cages depends on these environments, we obtain nine different frequencies. Both in the upper and lower panels for the M63 system, we see that the blue frequencies are distributed around the Raman spectrum 2915 cm^{-1}, while the red frequencies are between the Raman spectra 2905 cm^{-1} and 2915 cm^{-1}. The same situation holds for the M65 system. These histograms show that the C–H frequency of methane in a small cage is almost in agreement with the observed spectrum (2915 cm^{-1}), whereas the one in a large cage is higher than the observed spectrum (2905 cm^{-1}).

In Table 2, we show for the M63 and M65 systems the calculated frequency ν_1 of the A1 mode, averaged over the nine environments. The corresponding results from our 2nd paper are repeated in Table 2 for easy comparison to our new results. As depicted in the upper and the lower panels of Fig. 4(a and b), even though the cages are surrounded entirely or partly, the histograms have the same trend for both the small and large cages. This fact is reflected in the averaged values of Table 2. Specifically, the calculated values of methane in all small cages of the M63 system are averaged, and similarly for the large cages and for the M65 system. Furthermore, comparing the values in the corresponding

Table 2
Averaged frequency ν_1 of the A1 mode (in units of cm^{-1}).

M13 system		M63 system	
	Cages entirely enclosed		
Small cage	2916.6	Small cage	2915.0
		Large cage	2910.9
	Cages partly enclosed		
		Small cage	2915.1
Large cage	2911.2	Large cage	2910.9
M15 system		**M65 system**	
	Cages entirely enclosed		
		Small cage	2915.2
Large cage	2911.7	Large cage	2911.0
	Cages partly enclosed		
Small cage	2915.9	Small cage	2915.1
Large cage	2911.3	Large cage	2911.0

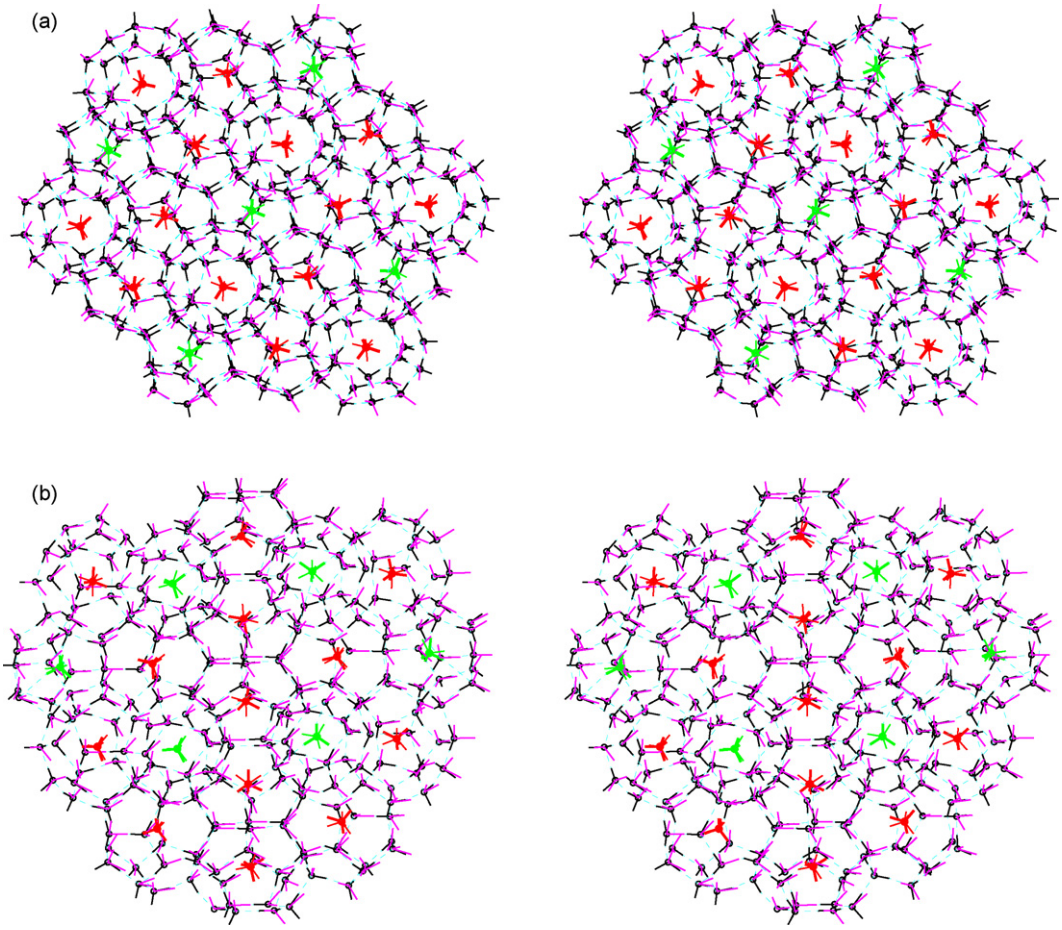

Fig. 3. (a) Stereo view for the M63 system. Waters of the 1st network with methanes (in bold green and bold red) of ran1 orientation are in black, while waters of the 2nd network with methanes (in thin green and thin red) of ran2 orientation are in magenta. For easy perception, only 19 cages of the 63 cages are displayed. Methanes in small cages are in green, while methanes in large cages are in red. In addition, hydrogens in the 2nd network deviate a little from the original sites for distinguishing from H-bondings in the 1st network. (b) Stereo view for the M65 system. Waters of the 1st network with methanes (in bold green and bold red) of ran1 orientation are in black, while waters of the 3rd network with methanes (in thin green and thin red) of ran3 orientation are in magenta. Only 19 cages of the 65 cages are depicted.

cages in both the M13 and M63 systems, we see that the values in the M63 system are a little lower than those in the M13 and are near to the observed Raman spectra. By comparing the M15 and M65, the same thing holds, although the differences are very small.

5. Discussion and conclusion

5.1. Our prediction is right or not?

In the 2nd paper, we say that "By constructing a model system larger than the present models, it should be possible to obtain frequencies in good agreement to the Raman spectra." Hence we tested this prediction using the two larger model systems, M63 and M65. The values calculated using the surface water fixed method are given in Table 2. As predicted in the 2nd paper, the values in the present models (M63 and M65) are nearer to the observed Raman spectra than the ones in the previous models (M13 and M15). Note specially that the values for the small cage go down somewhat and are in good agreement with the observed; values for the large cage go down, though not as much as expected.

Table 2 also shows that, even though a small or large cage is surrounded entirely or partly in both the M63 and M65 systems, the averaged frequency in the cage does not exhibit a difference due to a cage being wholly or partially surrounded by other cages. Instead, the values are almost the same, although the values of individual frequencies in the cage are different. This fact seems to be due to the larger model systems as depicted in Fig. 3(a and b). In the 2nd paper treating the smaller model M13 and M15 systems, we say that "our calculations show that methane in a cage partly surrounded by other cages has a lower frequency than the one fully surrounded, for both large and small cages, although this trend has not yet been definitely established experimentally". But this statement does not hold for the larger systems treated here. Our previous models were too small. The calculated average values for the M63 and M65 systems in Table 2 definitely do not exhibit differences depending on whether the cages are surrounded entirely or partly. Maybe experimental results from Raman or other methods would not show a difference due to the degree of enclosure. Our results seem to suggest that the larger the model, the more we imitate nature, and then the more we could learn from nature.

Up to now, we fixed movements of the surface oxygens of the model systems. To determine what is the same and what is different between the previous models (M13 and M15) and the present models (M63 and M65), we allow, as we did in the 2nd paper, surface oxygens to move within a volume radius r (Å), whose centre is at a fixed point. In Fig. 5(a and b), we show for small and large cages the frequency ν_1 of the A1 mode, averaged over three H-bonding network patterns with three random orientations plotted against the radius r (Å) parameter. Blue and red lines are for

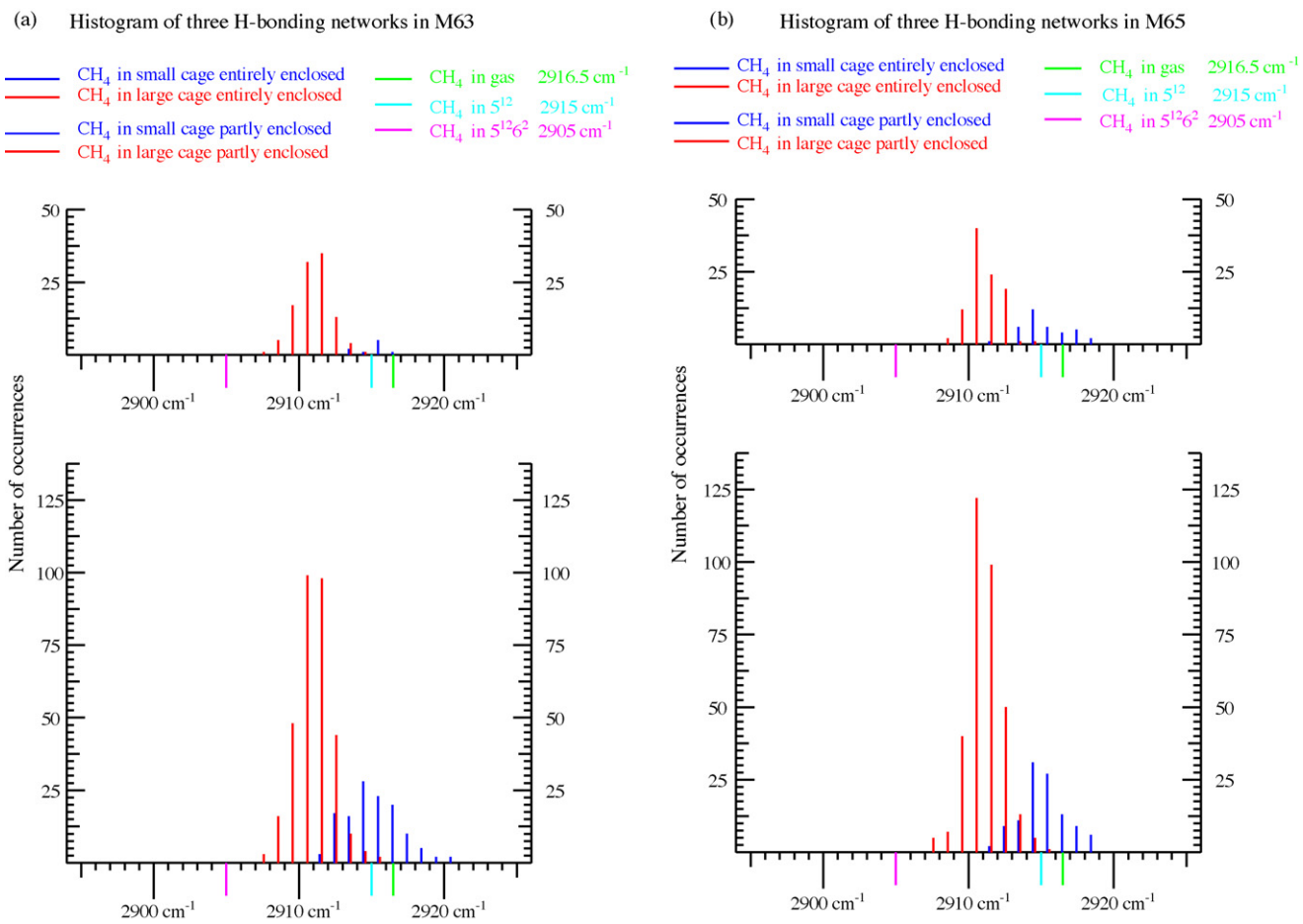

Fig. 4. Histogram of frequency ν_1 of the A1 mode. The frequency is counted as follows: e.g., a frequency ν_1 in the range of 2915.0 $cm^{-1} \leq \nu_1 < 2916$ cm^{-1} is counted as one at 2915.5 cm^{-1}. The frequencies are in blue for methanes in small cages, and in red for the large. Raman spectra are drawn in green, aqua and magenta. (a) For the M63 system. The upper part is provided for methanes entirely surrounded by the other cages: methanes in the M13 system. The total number of frequencies of blue is 1(small cage) × 9(environments), and the one of red is 12(large cages) × 9. The lower part is for methanes partly surrounded by the other cages: methanes newly added to the M13 system. The total number of blue is 14(small cages) × 9, and the one of red is 36(large cages) × 9. (b) For the M65 system. The upper part is for methanes entirely surrounded: methanes in the M15 system. The total number of blue is 4(small cages) × 9, and the one of red is 11(large cages) × 9. The lower part is for methanes partly surrounded: methanes newly added to the M15 system. The total number of blue is 12(small cages) × 9, and the one of red is 38(large cages) × 9.

the present model M63 and M65 systems, while aqua and magenta lines are for the previous model M13 and M15. Frequencies calculated at radius 0.0 Å are values given in Table 2. Frequencies are calculated up to radius 1.0 Å. Frequencies at infinite (inf.) radius are values obtained by the method with no constraints. Comparing the present and the previous models, the only thing the same is that frequencies at radius 0.0 Å for both the small and large cages are the lowest. As already described, frequencies of the present model are lower than the previous, regardless of whether the model is M63 or M65, or the cage is small or large. But, after the radius increases from 0.0 Å, the frequencies of the present model become generally higher than the previous.

At infinite radius, what are the minimum energy configurations? Fig. 9(a and c) in the 2nd paper show that the root-mean-square (rms) deviation of the oxygens in the minimum conformation from the corresponding oxygens in the X-ray structure was 0.758 Å for the 1st network of the model M13, and was 0.802 Å for the 1st network of the model M15. In the present model, the rms deviation is 0.878 Å for the 1st network of the model M63 and is 0.861 Å for the 1st network of the model M65. Thus, the conformation minimized with no constrains has a comparatively large rms deviation from the X-ray structure because the system deforms. At radius 0.0 Å, the minimum energy configurations of the present models fit as nicely with the X-ray structure as did the previous models; 0.042 Å for the 2nd network of the model M63, and 0.043 Å for the 3rd network of the model M65. We can say the structures of cages are almost retained at the X-ray crystallographic structure.

5.2. Refinement of the energy parameters

Considering the extent of the decrease in frequencies at radius 0.0 Å from the values of previous models to the present models (1.6 cm^{-1} down for small cage and 0.7 cm^{-1} down for large cage), even if we could construct larger models than the present models, we would not expect much further decrease in frequencies. Already the frequencies in the small cages are in good agreement with the Raman spectrum. Therefore, no further extension of the present models is necessary.

Instead, we look for another way to reduce the frequencies of large cages, while keeping the frequencies of small cages at their present values. One way would be to make refinements in the energy parameters. Many energy parameters exist in the energy terms expressed by Eq. (1). But as described more than once so far, the leading terms in the energy terms are the cubic anharmonic potential energy $V^{(3)}$ expressed in Eq. (2) and the H-bonding energy between methane hydrogen and water oxygen in the third term of right-hand side of Eq. (3).

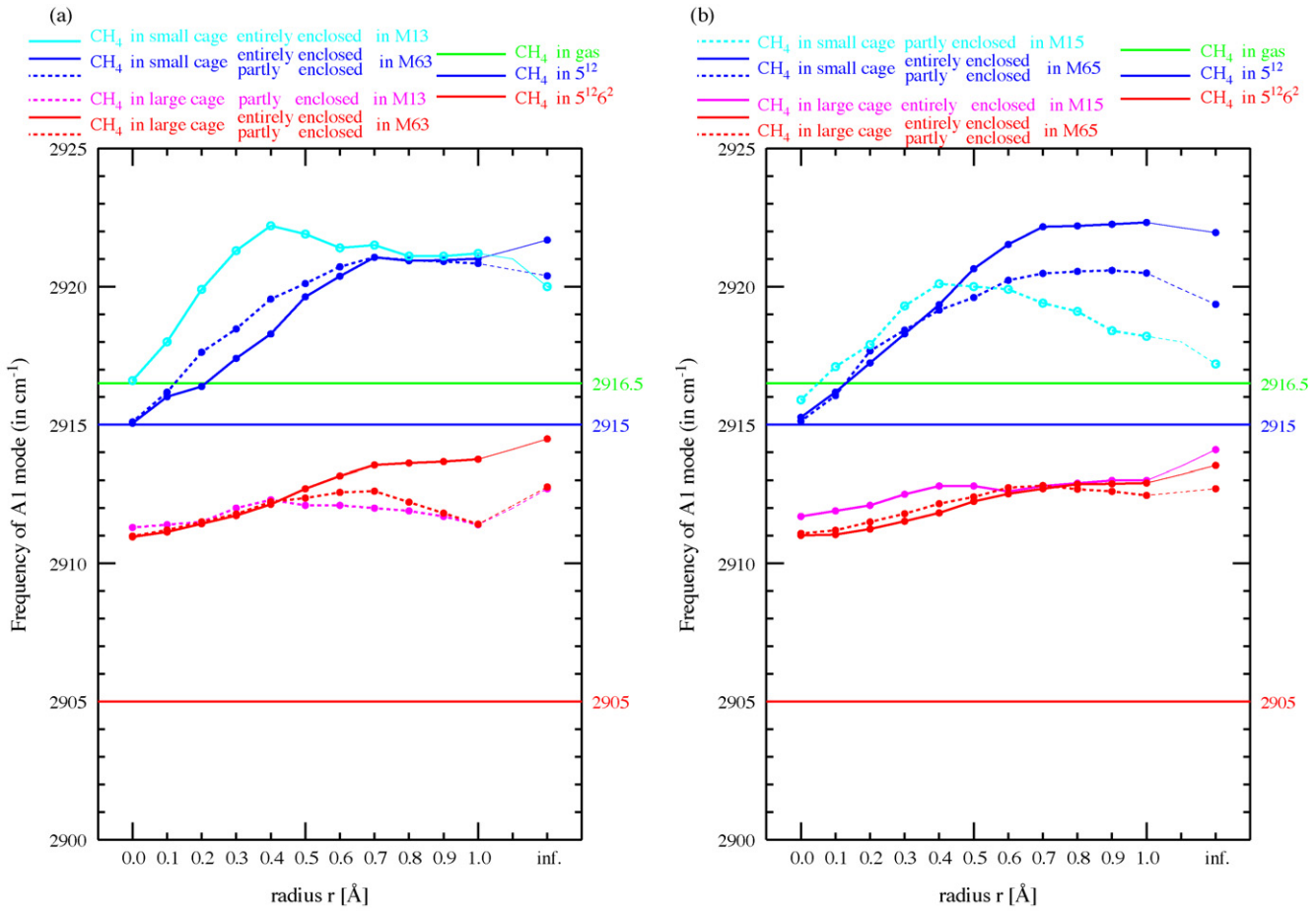

Fig. 5. Frequency ν_1 of the A1 mode are plotted against the radius r (Å) of oxygen movement. The blue lines indicate the frequencies of the small cage, whereas the red lines indicate the large cage. The green line shows the frequency in gaseous methane. The aqua line represents the frequency of the small cage in the M13 or M15 system, whereas the magenta line represents the large cage in the M13 or M15. (a) M13 and M63 systems. (b) M15 and M65 systems.

Let us first consider the anharmonic potential energy $V^{(3)}$, whose expression is represented by Eq. (A-2) in the 1st paper. We again show the equation below:

$$\begin{aligned}
6V^{(3)} = {} & f_{\mathrm{rrr}}(\Delta\rho_1^3;4) + 3f_{\mathrm{rrs}}(\Delta\rho_1^2\Delta\rho_2;12) \\
& + 6f_{\mathrm{rst}}(\Delta\rho_1\Delta\rho_2\Delta\rho_3;4) + 3f_{\mathrm{rr\alpha}}(\Delta\rho_1^2\Delta\alpha_{12};12) \\
& + 3f_{\mathrm{rr\beta}}(\Delta\rho_1^2\Delta\alpha_{23};12) + 6f_{\mathrm{rs\alpha}}(\Delta\rho_1\Delta\rho_2\Delta\alpha_{12};6) \\
& + 6f_{\mathrm{rs\beta}}(\Delta\rho_1\Delta\rho_2\Delta\alpha_{13};24) + 6f_{\mathrm{rs\omega}}(\Delta\rho_1\Delta\rho_2\Delta\alpha_{34};6) \\
& + 3f_{\mathrm{r\alpha\alpha}}(\Delta\rho_1\Delta\alpha_{12}^2;12) + 3f_{\mathrm{r\beta\beta}}(\Delta\rho_1\Delta\alpha_{23}^2;12) \\
& + 6f_{\mathrm{r\alpha\beta}}(\Delta\rho_1\Delta\alpha_{12}\Delta\alpha_{13};12) \\
& + 6f_{\mathrm{r\alpha\gamma}}(\Delta\rho_1\Delta\alpha_{12}\Delta\alpha_{23};24) \\
& + 6f_{\mathrm{r\gamma\delta}}(\Delta\rho_1\Delta\alpha_{23}\Delta\alpha_{24};12) \\
& + 6f_{\mathrm{r\alpha\omega}}(\Delta\rho_1\Delta\alpha_{12}\Delta\alpha_{34};12) + f_{\alpha\alpha\alpha}(\Delta\alpha_{12}^3;6) \\
& + 3f_{\alpha\alpha\beta}(\Delta\alpha_{12}^2\Delta\alpha_{13};24) + 3f_{\alpha\alpha\omega}(\Delta\alpha_{12}^2\Delta\alpha_{34};6) \\
& + 6f_{\alpha\beta\gamma}(\Delta\alpha_{12}\Delta\alpha_{13}\Delta\alpha_{14};4) \\
& + 6f_{\alpha\beta\delta}(\Delta\alpha_{12}\Delta\alpha_{13}\Delta\alpha_{23};4) \\
& + 6f_{\alpha\beta\omega}(\Delta\alpha_{12}\Delta\alpha_{13}\Delta\alpha_{34};12) \qquad (5)
\end{aligned}$$

where the values of the anharmonic internal coordinate force constant are given in Table A3 of the 1st paper. Of the 20 force constants in Eq. (5), the principal ones relating mainly to the C–H stretch frequency in methane are the first three force constants f_{rrr}, f_{rrs} and f_{rst}. Hence we would think these values should be treated as parameters.

Next, the H-bonding energy parameter between methane hydrogen and water oxygen is expressed as ε in the third term of Eq. (3) and is set at 75% of the strength of the H-bonding potential energy between waters. This energy parameter is also adjustable. Thus we will treat f_{rrr}, f_{rrs}, f_{rst} and the percent of the strength as four adjustable parameters.

With a set of new values of the four parameters, each of the nine assemblies for both the M63 and the M65 systems was energy minimized with the surface water fixed method. Again normal mode analysis was done on each of the nine assemblies. In the process of finding reasonable C–H stretch frequencies, the values of the four parameters were varied over a wide range. One set of new values that gave interesting results is listed in Table 3. With these values, the histograms of frequency ν_1 of the A1 mode considering three H-bonding network patterns and three random orientations both for the M63 and M65 systems are given in Fig. 6(a and b). Comparing these figures with Fig. 4(a and b), we see that the frequencies in large cages distributed around the Raman spectrum observation of 2905 cm^{-1}, unlike the histograms shown in Fig. 4(a and b), whereas the frequencies in small cages distributed around the Raman spectrum value of 2915 cm^{-1} in both figures. In Table 4, we show frequencies ν_1 of the A1 mode, averaged over three H-bonding network patterns with three random orientations. The averaged frequency in small cages is about 2913.6 cm^{-1}, which is a little lower than the Raman, while

Table 3
Four energy parameters newly chosen.

	Old parameters	New parameters
	In units of aJ/Å^3	
f_{rrr}	−17.60250	−18.48263
f_{rrs}	0.09375	−5.51650
f_{rst}	−5.88000	−5.58600
H-bond strength	75%	65%

the average frequency in large cages is about 2906.6 cm^{-1}, which is a little higher than the Raman.

If we apply these four new parameters to the previous model M13 and M15, what changes to the previous would happen? To see this, the calculated values are shown in the left side in Table 4, similar to Table 2. We see that the values calculated with the new parameters are better than the values with the old parameters. Considering the values for the model M63 and M65, we can at least say that we almost reach the Raman spectra with the new energy parameters, although not perfectly. The set of the energy parameters reported in this article is one possibility. If some of the $f_{rr\alpha}$, $f_{rr\beta}$ $f_{rs\alpha}$, $f_{rs\beta}$, $f_{rs\omega}$ [having the unit of aJ/(Å^2 rad)] of the anharmonic potential energy expressed in Eq. (5) were treated as additional adjustable parameters, it might be possible to obtain frequencies in better agreement with the Raman spectra. But we stop further extensions at present.

Here we give anisotropic thermal vibrations for each methane atom and each water atom, calculated with the set of the new energy parameters. For the carbon and hydrogen atoms of methane, the mean-square displacement matrix includes the nine normal vibrational modes [1], while for oxygen and hydrogen atoms of water this matrix includes the three normal vibrational modes. We depict the internal motions in the M63 and M65 systems in Fig. 7(a and b), respectively. In these figures we calculate the displacements that occur when each of the normal modes is thermally excited at 100 K.

Table 4
Averaged frequency ν_1 of the A1 mode, calculated with a set of new energy parameters (in units of cm^{-1}).

M13 system		M63 system	
	Cages entirely enclosed		
Small cage	2915.6	Small cage	2913.9
		Large cage	2906.7
	Cages partly enclosed		
		Small cage	2913.6
Large cage	2907.1	Large cage	2906.6
M15 system		**M65 system**	
	Cages entirely enclosed		
		Small cage	2913.3
Large cage	2907.6	Large cage	2906.5
	Cages partly enclosed		
Small cage	2914.9	Small cage	2913.9
Large cage	2907.0	Large cage	2906.7

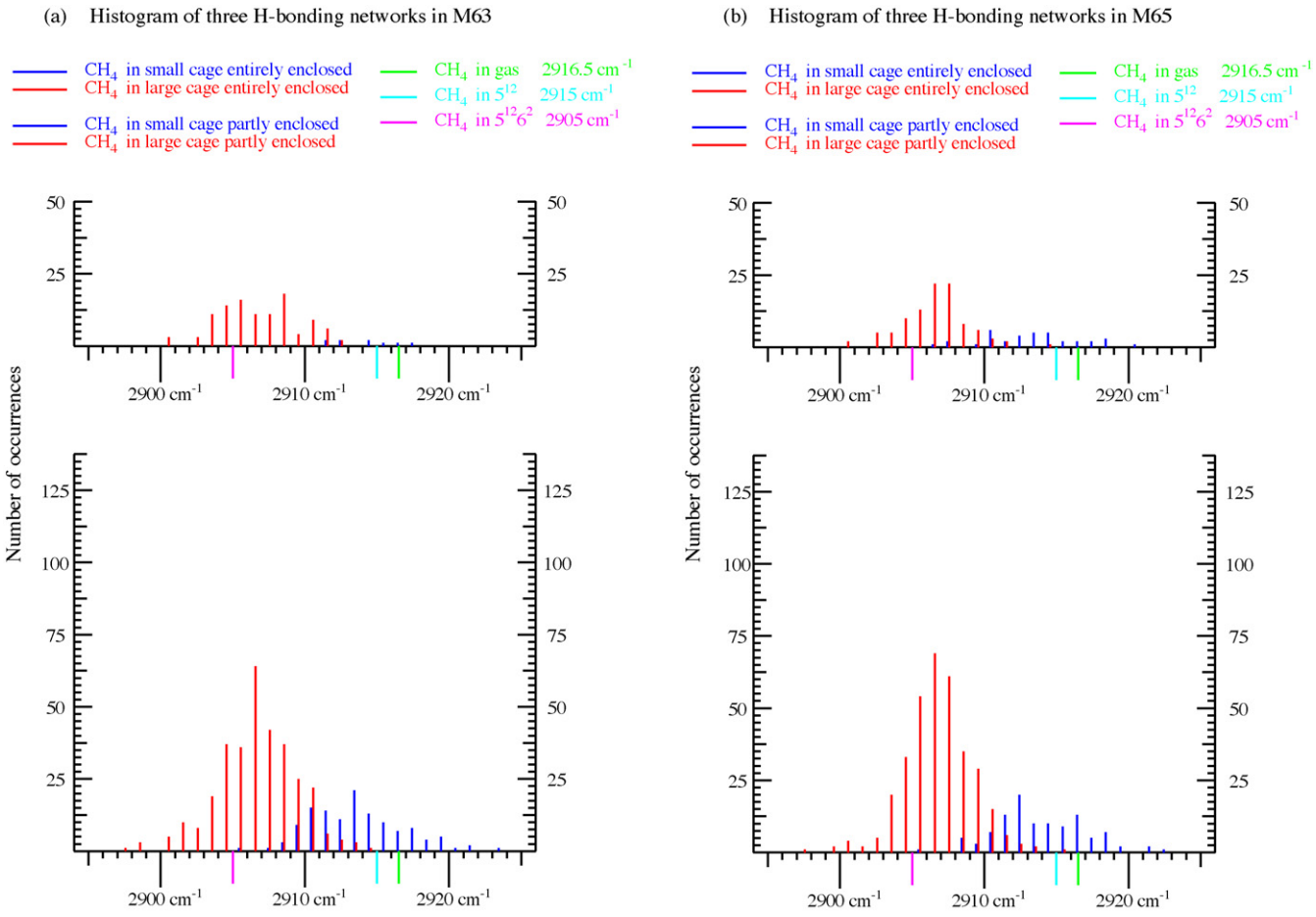

Fig. 6. Histogram of frequency ν_1 of the A1 mode, calculated with a set of the four new energy parameters. The legend is the same as for Fig. 4. (a) M63 system. (b) M65 system.

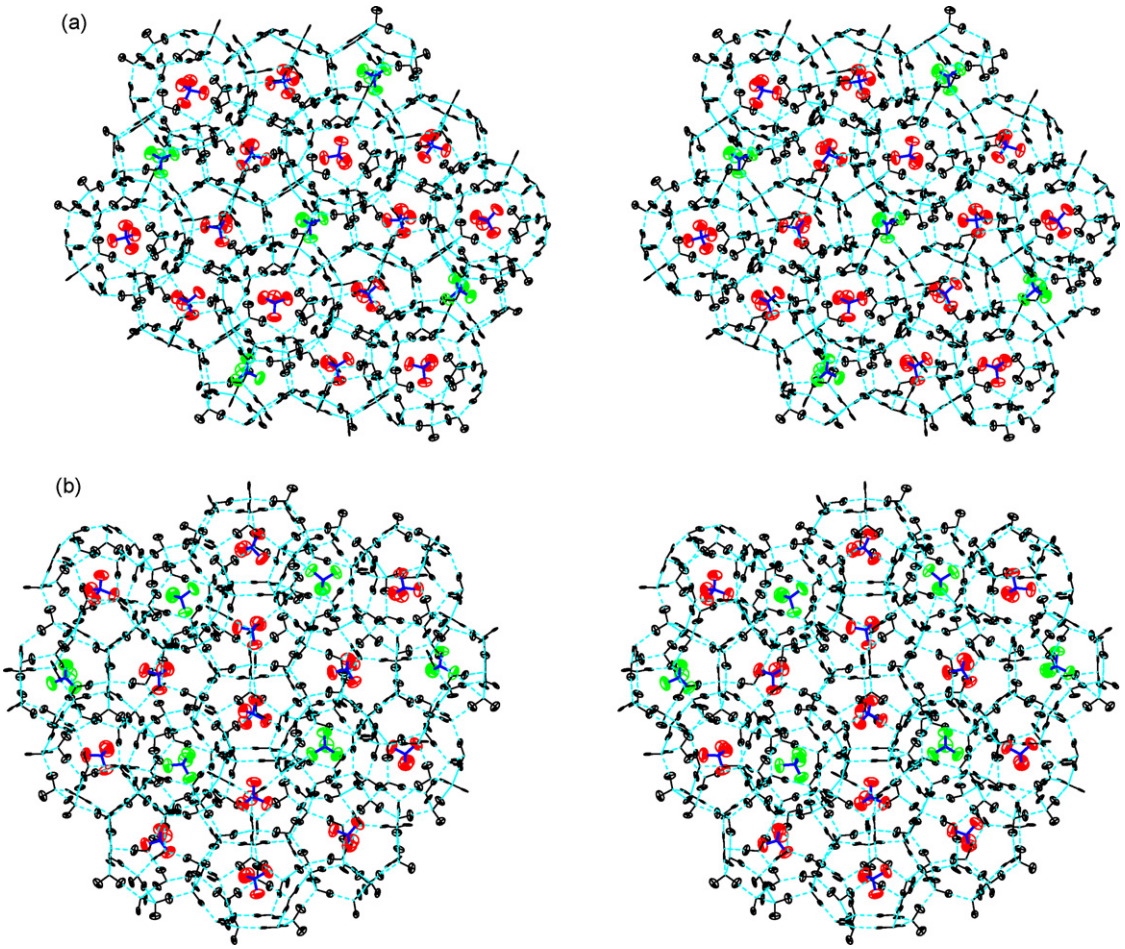

Fig. 7. Stereo view of internal motions of all atoms. The thermal ellipsoids of atoms (at 100% probability) are drawn with ORTEP [11] and are magnified 14.42^3 (=3000) times for easy recognition. Only 19 cages for each model system are chosen. The ellipsoids of hydrogen of methane in small cages are in green, whereas the ones in large cages are in red. The ellipsoids of carbon and the bonds of methane are in blue. (a) 2nd network with ran2 orientation in the M63 system. The configuration is the same as Fig. 3(a). (b) 1st network with ran1 orientation in the M65 system. The configuration is the same as Fig. 3(b).

5.3. What are essential differences between the small models and larger models?

First, from a quantitative point of view, let us compare the small models M13 and M15 with the larger models M63 and M65. From Figs. 1(a) and 2(a), we can estimate as follows: Each small model is generously approximated to be a sphere with radius about 11 Å, and also each larger model is approximated to be a sphere with radius about 18 Å. Next let us look at Fig. 7(a and b). If methanes in the cages were considered to be water molecules, these larger models correspond to 11 layers of H-bonding networks of waters at a maximum width of 36 Å. From Fig. 7(a and b) (or from Fig. 8(a and b) in the 2nd paper), the small models correspond to seven layers of H-bonding networks at a maximum width of 22 Å.

Second, from a qualitative point of view, let us see what happened to these small and larger models. As already described, we can see that in the case of the larger models, the average frequencies of A1 mode of methane are closer to the Raman spectra than the values from the small models. Furthermore, in the case of the larger models, the averaged frequency in the cage does not exhibit a difference due to a cage being wholly or partially surrounded by other cages. This fact is converse to results from the small models.

Hence, our computational results reveal there is danger of inadequate understandings or misunderstandings of nature arising from use of only the small model systems. The importance of studying the larger model systems as done here is that by removing the approximation inherent in small models it is possible to better understand the essence of nature. Scientists use models. The more realistic the model, the more likely we are able to discern the truth about nature.

In our study of H-bonding networks of waters, at least 11 layers of H-bonding network appear to be necessary to correctly understand hydrate methane, although more layers would be acceptable. To analyse at the atomic level the physical characteristics of a molecule in an aggregation of small molecules, the cluster should have a radius of at least about 18 Å. If our concerns were about electron distributions, maybe it would not be necessary or practical to use such a large model system. If our concerns were studies at the molecular level, it would depend on which properties were being investigated. At present, we cannot say any more. Other examples of studies that could be treated at the atomic level include internal motions of clathrates other than methane, stabilization of guest molecules in clathrates, internal motions in a drop of water, vibrations or stabilization of interstitial molecules in ice, or so on. As we extend our approach to other systems, we will establish how general our methodology is and where its usage is limited.

Last, in conclusion, the independent molecule model with the surface water fixed method almost matches the observed Raman spectra for both the small and the large cages. In addition, the energy minimized assembly almost fits the X-ray crystallographic structure. Our method moderately well reproduces one portion of the internal motions of methane hydrate in nature, even though

the models used are still small compared to the macroscopic scale. Dynamical structures of the methane hydrates other than structure I will be studied in the future.

References

[1] S. Yoshioki, Application of the independent molecule model to elucidate the dynamics of structure I methane hydrate, J. Mol. Graphics Modell. 25 (2007) 856–869.
[2] S. Yoshioki, Application of the independent molecule model to elucidate the dynamics of structure I methane hydrate: a second report, J. Mol. Graphics Modell. 26 (2008) 1353–1364.
[3] E.D. Sloan Jr., Clathrate Hydrates of Natural Gases, 2nd ed., Marcel Dekker Inc., New York, 1998 (Revised and expanded).
[4] R.K. McMullan, G.A. Jeffrey, Polyhedral clathrate hydrates. IX. Structure of ethylene oxide hydrate, J. Chem. Phys. 42 (1965) 2725–2732.
[5] A.K. Sum, R.C. Burruss, E.D. Sloan Jr., Measurement of clathrate hydrates via Raman spectroscopy, J. Phys. Chem. B 101 (1997) 7371–7377.
[6] I.-M. Chou, A. Sharma, R.C. Burruss, J. Shu, H. Mao, R.J. Hemley, A.F. Goncharov, L.A. Stern, S.H. Kirby, Transformations in methane hydrates, Proc. Natl. Acad. Sci. U.S.A. 97 (2000) 13484–13487.
[7] T. Uchida, R. Okabe, K. Gohara, S. Mae, Y. Seo, H. Lee, S. Takeya, J. Nagao, T. Ebinuma, H. Naria, Raman spectroscopic observations of methane-hydrate formation and hydrophobic hydration around methane molecules in solution, Can. J. Phys. 81 (2003) 359–366.
[8] D.L. Gray, A.G. Robiette, The anharmonic force field and equilibrium structure of methane, Mol. Phys. 37 (1979) 1901–1920.
[9] W.T. Raynes, P. Lazzeretti, R. Zanasi, A.J. Sadlej, P.W. Fowler, Calculations of the force field of the methane molecule, Mol. Phys. 60 (1987) 509–525.
[10] P.E. Gill, W. Murray, M.H. Wright, Practical Optimization, Academic Press, London, 1981, p. 105.
[11] C.K. Johnson, ORTEP: A Fortran Thermal Ellipsoid Plot Program, ORNL-3795, Oak Ridge National Laboratory, Oak Ridge, Tennessee, USA, 1965.